Published in final edited form as:
Circ Res. 2014 January 3; 114(1): 41–55. doi:10.1161/CIRCRESAHA.114.302500.

c-kit-Positive Cardiac Stem Cells Nested in Hypoxic Niches are Activated by Stem Cell Factor Reversing the Aging Myopathy

Fumihiro Sanada[1,2,3], **Junghyun Kim**[1,2,3], **Anna Czarna**[1,2,3], **Noel Yan-Ki Chan**[1,2,3], **Sergio Signore**[1,2,3], **Barbara Ogórek**[1,2,3], **Kazuya Isobe**[1,2,3], **Ewa Wybieralska**[1,2,3], **Giulia Borghetti**[1,2,3], **Ada Pesapane**[1,2,3], **Andrea Sorrentino**[1,2,3], **Emily Mangano**[1,2,3], **Donato Cappetta**[1,2,3], **Chiara Mangiaracina**[1,2,3], **Mario Ricciardi**[1,2,3], **Maria Cimini**[1,2,3], **Emeka Ifedigbo**[2,4], **Mark A. Perrella**[2,4,5], **Polina Goichberg**[1,2,3], **Augustine Choi**[2,4], **Jan Kajstura**[1,2,3], **Toru Hosoda**[1,2,3], **Marcello Rota**[1,2,3], **Piero Anversa**[1,2,3], and **Annarosa Leri**[1,2,3]

[1]Department of Anesthesia, Brigham and Women's Hospital, Harvard Medical School, Boston, MA 02115, USA

[2]Department of Medicine, Brigham and Women's Hospital, Harvard Medical School, Boston, MA 02115, USA

[3]Division of Cardiovascular Medicine, Brigham and Women's Hospital, Harvard Medical School, Boston, MA 02115, USA

[4]Division of Pulmonary and Critical Care Medicine, Brigham and Women's Hospital, Harvard Medical School, Boston, MA 02115, USA

[5]Division of Newborn Medicine, Brigham and Women's Hospital, Harvard Medical School, Boston, MA 02115, USA

Abstract

Rationale—Hypoxia favors stem cell quiescence, while normoxia is required for their activation; but whether cardiac stem cell (CSC) function is regulated by the hypoxic/normoxic state of the cell is currently unknown.

Objective—A balance between hypoxic and normoxic CSCs may be present in the young heart, although this homeostatic control may be disrupted with aging. Defects in tissue oxygenation occur in the old myocardium, and this phenomenon may expand the pool of hypoxic CSCs, which are no longer involved in myocyte renewal.

Methods and Results—Here we show that the senescent heart is characterized by an increased number of quiescent CSCs with intact telomeres that cannot reenter the cell cycle and form a differentiated progeny. Conversely, myocyte replacement is controlled only by frequently dividing CSCs with shortened telomeres; these CSCs generate a myocyte population that is chronologically young but phenotypically old. Telomere dysfunction dictates their actual age and mechanical behavior. However, the residual subset of quiescent young CSCs can be stimulated in situ by stem cell factor reversing the aging myopathy.

Conclusions—Our findings support the notion that strategies targeting CSC activation and growth interfere with the manifestations of myocardial aging in an animal model. Although

Address correspondence to: Dr. Annarosa Leri Departments of Anesthesia and Medicine Division of Cardiovascular Medicine Brigham and Women's Hospital Harvard Medical School 75 Francis Street Boston, MA 02115 USA Tel: 617-525-8174 Fax 617-264-6320 aleri@partners.org.

DISCLOSURES None.

caution has to be exercised in the translation of animal studies to human beings, our data strongly suggests that a pool of functionally-competent CSCs persists in the senescent heart and this stem cell compartment can promote myocyte regeneration effectively, correcting partly the aging myopathy.

Keywords

Cardiac stem cells; hypoxia; myocardial aging; stem cell factor

INTRODUCTION

In the myocardium, c-kit-positive cardiac stem cells (CSCs) are clustered in interstitial microdomains where they are connected by gap and adherens junctions to the supporting cells, i.e., cardiomyocytes and fibroblasts.[1] In the young heart, asymmetric growth kinetics of CSCs maintains their pool and promotes the generation of an adequate differentiated progeny.[2] With aging, the pool of stem cells expressing the senescence-associated protein $p16^{INK4a}$ increases, reducing the number of functionally-competent CSCs.[3,4] Apoptosis is restricted to $p16^{INK4a}$-positive CSCs,[3] but this process may be inefficient leading to the accumulation of old CSCs. A shift in the balance between actively dividing and senescent CSCs may generate dysfunctional niches, altering the critical role that CSCs have in the homeostasis of the aged myocardium. Deregulation of niche function may create abnormal sites of cardiomyogenesis; old CSCs form myocytes, which inherit the shortened telomeres of the mother cells, rapidly acquiring the senescent cell phenotype.[3,4] These variables are major determinants of the aging myopathy.[3–5]

Stem cell niches in the bone marrow are characterized by low oxygen tension[6] that offers a selective advantage to stem cells favoring their quiescent, undifferentiated state.[7,8] A similar mechanism may be operative in the myocardium, and CSC behavior may be regulated by the O_2 gradient within the tissue. The long-term preservation of the CSC compartment may require a hypoxic milieu, although physiological normoxia may be necessary for active cardiomyogenesis. A balance between hypoxic and normoxic CSCs may be present in the young heart, ensuring tissue homeostasis and myocyte renewal. Conversely, this balance may be disrupted in the old myocardium in which defects in tissue oxygenation and enhanced fibroblast accumulation[9] may increase the number of hypoxic foci. CSCs nested in this microenvironment are unable to reenter the cell cycle and divide. By necessity, normoxic CSCs are forced to undergo intense proliferation and differentiation with progressive telomere erosion, and formation of senescent dysfunctional cardiomyocytes.[10] Hypoxic CSCs may comprise a cell population with intact telomeres and significant growth reserve, which following activation may reverse partly the cardiac senescent phenotype.

METHODS

A detailed description of the experimental procedures is provided in the Online Supplement.

Hypoxic and normoxic CSCs

Protocols were approved by the institutional IACUC. Male C57BL/6 mice at 3, 24, and 30 months of age were injected i.p. with the hypoxic probe pimonidazole (Pimo).[11] Two hours later, mice were sacrificed and the heart was formalin-fixed. The presence of Pimo in CSCs was determined by immunolabeling.

Nitroreductase activity, mitochondrial content and ΔΨ

The heart of Pimo-injected mice at 3 months of age was enzymatically dissociated, and c-kit-positive CSCs were analyzed by flow-cytometry. FACS-sorted CSCs were incubated with nitroblue tetrazolium to detect nitroreductase enzymatic activity. The fluorescent probes MitoTracker Green FM and tetramethylrhodamine ethyl ester (TMRE) were employed to evaluate, respectively, mitochondrial content and membrane potential in CSCs. The distribution of Pimo in CSCs was assessed by immunolabeling and confocal microscopy.

Functional properties of pimonidazole-positive and pimonidazole-negative CSCs

CSCs isolated from mice at 3 and 30 months of age[1,3] were fixed, permeabilized, and incubated with antibodies against c-kit, Pimo, Ki67, GATA4, Nkx2.5, and $p16^{INK4a}$.

Capillary density

Sixty μm thick sections were obtained from hearts of mice at 3 and 26–30 months of age. The distance between hypoxic and normoxic CSCs and the closest endothelial cell (EC), and the capillary density per mm^2 of myocardium were determined.[12]

Depletion of hypoxic CSCs

Mice at 3 and 30 months of age were injected daily with the cytotoxic agent tirapazamine, TPZ; 30 mg/kg b.w.,[13] and received Pimo 2 hours prior to sacrifice. The number of CSCs,[12,14] the percentage of pimonidazole-positive CSCs ($Pimo^{pos}$-CSCs) and pimonidazole-negative CSCs ($Pimo^{neg}$-CSCs), and the fraction of cycling and committed CSCs were then measured.

Long-term label retaining assay

Mice at 3 months of age were injected i.p. with BrdU at 12 hours intervals for 7 days. One group of animals was sacrificed one hour after the last administration of the halogenated nucleotide (pulse). Two additional groups of mice were similarly treated and sacrificed after a chase period of 2 and 5 months.[1–3] The fluorescence intensity of BrdU in CSCs was measured by confocal microscopy.

Telomere length

This parameter was evaluated by Q-FISH and confocal microscopy in CSCs and cardiomyocytes isolated from hearts at 3 and 30 months of age.

Hyperoxia and SCF administration

Mice at 26 months of age were kept in hyperoxic chambers, 70% O_2, for 1 and 7 days. $Pimo^{pos}$- and $Pimo^{neg}$-CSCs were measured by flow-cytometry. The heart of mice at 26–30 months of age was injected at 3–4 different sites with 1 μg stem cell factor (SCF) or PBS and sacrificed at 6, 24 and 48 hours, and 21 days. Mice killed at 2 and 21 days received daily injections of BrdU, 10 mg/kg b.w., and the percentage of CSCs and cardiomyocytes positive for BrdU was measured by confocal microscopy.[1,3]

Myocyte volume and number

Sections, 40 μm thickness, were stained by α-sarcomeric actin, laminin and connexin 43. Optical sections 1 μm apart were collected and images were converted into 3D structures to measure the proportion of mono-, bi-, and multi-nucleated myocytes, and their volume and number.[12]

Data analysis

Data are presented as mean±SD. Significance between two groups was determined by unpaired two-tailed Student's t-test. For multiple comparisons, the ANOVA test was employed.

RESULTS

Hypoxic and normoxic CSC niches are present in the heart

Oxygen tension in the heart varies from 18 to 35 mmHg reflecting physiological normoxia.[15] The small size of the niches, their scattered distribution in the myocardium, and the complexity to identify these structures in vivo, make it impossible to measure with electrodes O_2 level in cardiac niches. Therefore, the uptake of the hypoxic marker pimonidazole (Pimo) was introduced to define O_2 content in CSCs. Pimo diffuses across the plasma-membrane and undergoes bioreduction by cytoplasmic nitroreductases when O_2 level is lower than 10 mmHg, or 1.3%. Pimo intermediates bind to macromolecules allowing the detection of intracellular hypoxia by immunocytochemistry.[11]

Three variables of CSC function were measured to validate the specificity of Pimo labeling: activity of nitroreductases,[16] aggregate mitochondrial volume, and transmembrane potential of the inner mitochondrial membrane ($\Delta\Psi$).[17,18] The first parameter was determined by the nitroblue tetrazolium chloride (NBT) assay[11] that detects the activity of hypoxia-dependent and hypoxia-independent reductases. By this approach, the possibility that Pimo-positive ($Pimo^{pos}$) and Pimo-negative ($Pimo^{neg}$) CSCs had different enzyme activity was tested. The second and third parameters were measured utilizing fluorescent probes and FACS. This was done because differences in the mitochondrial compartment and $\Delta\Psi$ are strictly related to the rate of mitochondrial respiration, allowing the recognition of differences in O_2 consumption and in the oxidative state of the cell.

Nitroreductase activity was comparable in $Pimo^{pos}$ and $Pimo^{neg}$ CSCs (Online Figure IA), as was the mitochondrial volume. In the latter assay, CSCs were divided into two categories according to the level of intensity of the Mito Tracker probe, and the localization of Pimo in these two CSC classes was determined. The fraction of $Pimo^{pos}$-cells was identical regardless of the degree of mitochondrial content (Online Figure IB). However, $Pimo^{pos}$-CSCs were distributed predominantly in the cell group with low $\Delta\Psi$ (Online Figure IC). Moreover, human CSCs cultured at 1%, 5%, 10%, and 21% O_2 were $Pimo^{pos}$ only in the presence of 1% O_2 (Online Figure IIA). Thus, Pimo labeling was consistent with the identification of hypoxic CSCs.

The thymus, an organ characterized by a microenvironment with O_2 content less than 10 mmHg, was employed to establish the efficiency of Pimo in labeling hypoxic cells in vivo (Online Figure IIB). Pimo was injected intraperitoneally 2 hours prior to sacrifice and the proportion of hypoxic and normoxic CSCs in the atria, base-mid-region (Base-MR), and apex of the left ventricle (LV) was measured by confocal microscopy in mice at 3, 24 and 30 months of age. $Pimo^{pos}$-hypoxic-CSCs ($Pimo^{pos}$-CSCs) and $Pimo^{neg}$-normoxic-CSCs ($Pimo^{neg}$-CSCs) were seen in all anatomical areas (Figures 1A and 1B).

Myocytes and fibroblasts operate as supporting cells within the CSC niches[1] so that the presence of Pimo in these cells was determined to define the hypoxic state of the microenvironment of the niches. Fibroblasts in proximity of $Pimo^{pos}$-CSCs were consistently labeled, while cardiomyocytes were always Pimo-negative (Figure 1C). This observation raised the question whether cardiomyocytes adjacent to $Pimo^{pos}$-CSCs were normoxic or in a state of relative hypoxia. Two indices of the molecular response to hypoxia, HIF-1α and its downstream effector carbonic anhydrase IX (CAIX),[6] were

introduced to identify potential defects in cell oxygenation. Importantly, HIF-1α but not CAIX was detected in cardiomyocytes contiguous to Pimo-positive CSCs; however, CAIX was present in Pimo-positive CSCs (Figure 1D and 1E). Pimo-negative CSCs labeled by HIF-1α were found, suggesting that these cells were relatively hypoxic but did not reach the severe hypoxic state associated with CAIX and Pimo labeling (Figure 1F). The partial overlapping in the distribution of these three markers of hypoxia in cardiac niches is consistent with findings in tumor cells.[19,20] The upregulation of the nuclear transcription factor HIF-1α has also been observed in cells with O_2 content higher than 1%, although the activation of the transmembrane protein CAIX appears to be limited to cells with O_2 content lower than 1%. Thus, the mouse heart is characterized by hypoxic and normoxic niches, which may have a distinct role in organ homeostasis, tissue repair, and myocardial aging.

The number of hypoxic CSC Niches increases with age

At 3 months of age, the number of CSCs/mm^3 of myocardium was similar in the atria and apex, and lower at the Base-MR. From 3 to 30 months, the number of CSCs increased 53%, 103%, and 86% in the atria, Base-MR, and apex, respectively (Online Figure IIC). At 3 months, $Pimo^{pos}$-CSCs comprised only 27–35% of the stem cell population, but reached a value of 56–65% at 30 months. Conversely, the fraction of $Pimo^{neg}$-CSCs decreased with age (Figure 2A). The senescent heart at 30 months contained in all regions a comparable number of $Pimo^{pos}$-CSCs/mm^3 of myocardium which exceeded the pool of $Pimo^{neg}$-CSCs (Figure 2B). At 30 months, the ratio of $Pimo^{pos}$-CSCs-to-$Pimo^{neg}$-CSCs was 1.4, 1.9, and 1.3 in the atria, Base-MR, and apex, respectively. When possible, mice at 30 months of age were evaluated separately. However, the low survival rate of mice at 30 months imposed on us to include in some experiments animals from 24–30 months.

To establish whether hypoxia prevented cell cycle reentry, the localization of Ki67 was evaluated in $Pimo^{pos}$- and $Pimo^{neg}$-CSCs. $Pimo^{pos}$-CSCs did not express Ki67. At all ages, in the three regions of the heart, Ki67 was restricted to $Pimo^{neg}$-CSCs (Figure 2C). Thus, aging increases the number of hypoxic non-dividing CSCs, a process that may interfere with organ homeostasis and repair.

Capillaries and $Pimo^{pos}$-CSCs

The oxygenation of the niches is regulated by the distance between CSCs and the closest capillary.[12,21] This parameter was measured by two-photon microscopy at the LV Base-MR of 3 and 24–30 month-old mice, 2 hours after Pimo injection. The myocardium was fixed and 60 μm thick sections were stained for c-kit and Pimo; coronary capillaries were identified by isolectin. The distance between the closest capillary and $Pimo^{pos}$-CSCs at 3 and 24–30 months of age varied from 10.4 μm to 12.9 μm; these values were significantly higher than those found between the closest capillary and $Pimo^{neg}$-CSCs, ranging from 5.6 μm to 7.6 μm (Figure 2D). The numerical density of capillaries per mm^2 of myocardium[12] within a radius of 30 μm from $Pimo^{pos}$- and $Pimo^{neg}$-CSCs was similar in both CSC subsets in the young heart (not shown). Capillary density decreased with age in a comparable manner in both CSC classes but did not reach statistical significance. The preservation of capillary density in the adjacent myocardium may explain the lack of severe hypoxia in myocytes distributed in proximity to hypoxic niches. Thus, the increase in diffusion distance for O_2 is viewed as one of the factors implicated in the induction of CSC quiescence, although cell autonomous mechanisms may also be involved.

$Pimo^{pos}$-CSCs and $Pimo^{neg}$-CSCs are functionally connected

To define the effects of hypoxia and normoxia on the division and differentiation of CSCs, these cells were isolated from 3 and 30 month-old mice and analyzed by FACS. Cells were depleted with a CD45-antibody to exclude bone marrow cells and mast-cells. The small

fraction of c-kit-positive-CD45-positive cells was Pimo^{neg} and normoxic (Online Figure III); this finding is consistent with the increase in O_2 content in committed hematopoietic stem cells (HSCs).[7]

Replicating CSCs were detected by Ki67, and GATA4 and Nkx2.5 were used as markers of the myocyte lineage. At 3 months, largely quiescent, lineage-negative Pimo^{pos}-CSCs comprised 38% of the population (Figure 3A and 3B), a value comparable to the results obtained in myocardial sections (see Figure 2A). Cycling and early committed CSCs, positive for Ki67, GATA4 and Nkx2.5, were predominantly restricted to the Pimo^{neg} pool (Figure 3A and 3B). At 30 months, quiescent, lineage-negative Pimo^{pos}-CSCs accounted for 65% of the cells. Again, dividing and differentiating cells were primarily confined to Pimo^{neg}-CSCs (Figure 3C and 3D). Thus, Pimo^{pos}-CSCs increase with age, and intracellular hypoxia conditions their quiescent state, while normoxia favors CSC growth and commitment.

A critical question was whether Pimo^{pos}- and Pimo^{neg}-CSCs are independent or functionally interrelated cell populations. To determine whether the loss of hypoxic Pimo^{pos}-CSCs triggered a response from the pool of normoxic Pimo^{neg}-CSCs, the cytotoxic agent tirapazamine (TPZ) was used.[13,22] TPZ kills hypoxic cells with O_2 content less than 1.3%. TPZ is activated by cytoplasmic reductases resulting in the generation of reactive oxygen species (ROS), DNA damage and apoptosis.[13,22] Following a single TPZ injection, 3 and 30 month-old mice were sacrificed 24 hours later (day 1). Two additional groups of mice received TPZ daily for 4 days and were killed one day (day 5) and 8 days (day 12) later. In all cases, Pimo was given 2 hours prior to sacrifice, and the thymus was used as a positive control (Online Figure IV).

To define whether TPZ had a detrimental effect on ventricular performance, cardiac hemodynamics was measured at day 12 in young and old mice. Left ventricular end-diastolic pressure (LVEDP), LV systolic pressure (LVSP), and positive and negative LV d*P*/d*t* were not changed by TPZ in either animal group. However, myocardial aging resulted in a severe depression in systolic and diastolic function (Online Figure V).

In 3 month-old mice at day 1, the fraction of Pimo^{pos}-CSCs decreased from 38% to 13%, while the fraction of Pimo^{neg}-CSCs increased from 62% to 87% (Figure 4A). At day 5, the CSC pool was reduced by 42% from 152 to 89 CSCs/mm^3 of myocardium (P=0.03). However, the percentage of Pimo^{pos}-CSCs returned to nearly its baseline value, 32%, as did the category of Pimo^{neg}-CSCs, 68% (Figure 4A). These proportions were maintained at day 12 (Figure 4A). In the senescent heart at 30 months, Pimo^{pos}- and Pimo^{neg}-CSCs accounted for 65% and 35% of the population, respectively (Figure 4A). One day after a single injection of TPZ (day 1), the fraction of Pimo^{pos}-CSCs decreased 62% and Pimo^{neg}-CSCs predominated (Figure 4A). At day 5, a 66% decrease in the CSC category occurred, from 306 to 106 CSCs/mm^3 of myocardium (P=0.001). Moreover, at day 5 and 12, the fraction of Pimo^{pos}-CSCs remained relatively constant averaging 29%.

In young mice, there were no changes in the fraction of cycling and differentiating Pimo^{pos}- and Pimo^{neg}-CSCs at day 1 (Figure 4B and 4C). However, the percentage of cycling Pimo^{neg}-CSCs increased 3-fold at day 5, from 4.8% at day 1 to 15% (Figure 4B). Since the proportion of cycling Pimo^{pos}-CSCs did not differ from that seen at baseline and at day 1, these data suggest that the newly-formed Pimo^{neg}-CSCs contributed to the reconstitution of the compartment of Pimo^{pos}-CSCs in the organ. This conclusion is supported by the decrease in lineage specification of Pimo^{neg}-CSCs at day 5 (Figure 4C).

The minimal level of expression of GATA4 and Nkx2.5 in Pimo^{neg}-CSCs at day 5 is consistent with the notion that these cells divided symmetrically generating two daughter stem cells, which were involved in the restoration of hypoxic niches within the adult heart. However, at day 12, the commitment of Pimo^{neg}-CSCs was higher than that seen at the earlier interval, while the fraction of Ki67-positive cells decreased by 73%. Thus, Pimo^{neg}- and Pimo^{pos}-CSCs were slowly reestablishing their physiological behavior based on the critical role that Pimo^{neg}-CSCs appear to have in the restoration of the pool of quiescent CSCs within the healthy myocardium. In old mice, a 39% increase in cycling Pimo^{neg}-CSCs was seen at day 5 in the absence of cell commitment (Figure 4B and 4C), reflecting an attempt to expand their own pool that was severely affected by age.

Thus, depletion of Pimo^{pos}-CSCs in the young heart appears to activate a population replacement process[23] involving replication of Pimo^{neg}-CSCs, which partially reconstitute the hypoxic CSC pool. However, depletion of Pimo^{pos}-CSCs in the old heart results in growth activation of Pimo^{neg}-CSCs, which restores partly the balance between these two CSC compartments lost with physiological aging.

Pimo^{pos}-CSCs have longer telomeres

With cell multiplication, chromosomal ends lose telomeric repeat sequences ultimately resulting in replicative senescence and apoptosis.[24] Despite the high level of telomerase activity, rapidly dividing CSCs undergo telomere erosion,[14] while quiescence protects telomere length and CSC growth. Long-term repopulating CSCs may retain relatively intact telomeres that sustain their proliferative reserve with aging. Following activation, this stem cell class may rejuvenate partly the old heart, since the long telomeres of the mother cell are inherited by the derived progeny, a parameter that is coupled with the integrity of the mechanical and electrical properties of myocytes.[10]

To test this possibility, mice at 3 and 30 months of age were exposed to Pimo; after enzymatic digestion of the myocardium, Pimo^{pos}- and Pimo^{neg}-CSCs were FACS-sorted (Online Figure VI), and ventricular myocytes were collected by differential centrifugation. Telomere length was then measured in these cells by Q-FISH (Figure 5A). Moreover, the expression of the senescence-associated protein p16^{INK4a}, which prevents the reentry of stem cells into the cell cycle,[25] was determined in CSCs.

In the young heart, the distribution of telomere lengths in Pimo^{pos}-CSCs was shifted to the right to values higher than those in Pimo^{neg}-CSCs. Cardiomyocytes showed telomeres shorter than in Pimo^{pos}- and Pimo^{neg}-CSCs (Figure 5B). The difference in telomere length between Pimo^{pos}- and Pimo^{neg}-CSCs increased in the senescent heart; again, cardiomyocytes carried significantly shorter telomeres than CSCs. Telomere length in Pimo^{pos}-CSCs did not decrease with age, while a 43% and 46% reduction in telomere length occurred in Pimo^{neg}-CSCs and myocytes, respectively (Figure 5C).

At 3 and 30 months, the fraction of Pimo^{neg}-CSCs expressing p16^{INK4a} was, respectively, 6-fold and 2.7-fold higher than in Pimo^{pos}-CSCs (Figure 5D). Thus, Pimo^{pos}-CSCs possess long telomeres, a property that largely persists in the senescent heart where 74% of this CSC class can divide and create a specialized progeny. In contrast, the majority of Pimo^{neg}-CSCs experiences telomere erosion with age, and only a small fraction, 30%, retains the ability to replicate and differentiate.

Hypoxic CSCs have properties of long-term label retaining cells

To determine whether Pimo^{pos}-CSCs represent the compartment of slowly dividing stem cells, a label retaining assay was performed in 3 month-old mice.[1] The pulse-period consisted of 14 injections of BrdU given at 12-hour intervals for 7 days. One group of mice

was then sacrificed, while two additional animal groups were killed, respectively, 2 and 5 months later. The fluorescence intensity of BrdU in Pimo^{pos}- and Pimo^{neg}-CSCs was measured by confocal microscopy.[1–3] Fluorescent levels >1,000 units (pixel × average intensity) were recorded; tissue autofluorescence, together with the signal generated by the irrelevant antibody used as a negative control for BrdU staining, was at most 900 units (Online Figure VII). BrdU intensity varying from 1,000–3,999 units and from 4,000–10,000 units was assigned to dimly-labeled and brightly-labeled cells, respectively (Figure 6A through 6C); low fluorescence reflected CSCs that underwent several divisions, while high fluorescence indicated CSCs which proliferated rarely.

At 7 days, and 2 and 5 months, the percentage of BrdU-labeled Pimo^{neg}-CSCs was similar in atria, Base-MR and apex, averaging 45% (Figure 6A through 6C). At 7 days, the fraction of BrdU-labeled Pimo^{pos}-CSCs was comparable in the three anatomical regions averaging 11%. However, at 2 months, BrdU-labeled Pimo^{pos}-CSCs reached 30% and 32% at the Base-MR and apex, respectively. From 2 to 5 months, BrdU-labeled Pimo^{pos}-CSCs increased to 57% at the apex; there was no further increase at the Base-MR. The fraction of BrdU-positive Pimo^{pos}-CSCs in the atria did not increase at 2 and 5 months (Figure 6C); thus, CSCs experienced a minimal number of divisions in this region.

Subsequently, the proportion of highly proliferating (dim), and rarely dividing (bright) Pimo^{neg}-and Pimo^{pos}-CSCs was determined. At 7 days, BrdU-bright Pimo^{neg}-CSCs in the atria, Base-MR and apex averaged 30%. BrdU-dim Pimo^{neg}-CSCs were higher in number at the Base-MR and apex, 19%, than in the atria, 5% (Figure 6D). At 2 and 5 months, BrdU-bright Pimo^{neg}-CSCs were essentially undetectable in all regions. However, BrdU-dim Pimo^{neg}-CSCs increased to 44% at 2 and 5 months. The population of BrdU-negative Pimo^{neg}-CSCs remained relatively constant at 7 days, and 2 and 5 months averaging 55% (Figure 6D). Thus, a large fraction of Pimo^{neg}-CSCs divided frequently over a period of 5 months.

The growth kinetics of Pimo^{pos}-CSCs differed from that of Pimo^{neg}-CSCs. At 7 days, throughout the heart, BrdU-bright Pimo^{pos}-CSCs included 11% of the population, and BrdU-dim Pimo^{pos}-CSCs were undetectable (Figure 6E). At 2 months, BrdU-bright Pimo^{pos}-CSCs remained constant in the atria, Base-MR and apex averaging 10%. BrdU-dim Pimo^{pos}-CSCs were not found in the atria, but appeared at the Base-MR and apex comprising 24% of the cells. From 2 to 5 months, BrdU-bright Pimo^{pos}-CSCs in the atria did not change, but a small pool, 9%, of BrdU-dim Pimo^{pos}-CSCs became apparent (Figure 6E). Conversely, at the Base-MR, BrdU-bright Pimo^{pos}-CSCs increased 2-fold, from 7% to 14%, while BrdU-dim Pimo^{pos}-CSCs remained constant, ~20%. From 2 to 5 months, no changes occurred in the fraction of BrdU-bright Pimo^{pos}-CSCs in the apex, although BrdU-dim Pimo^{pos}-CSCs increased from 24% to 52% (Figure 6E).

Importantly, BrdU-negative Pimo^{pos}-CSCs did not vary in the atria from 7 days to 2 and 5 months averaging 88%. However, from 7 days to 5 months, BrdU-negative Pimo^{pos}-CSCs decreased from 86% to 68% at the Base-MR, and from 92% to 43% at the apex (see Figure 6C). Collectively, these data suggest that Pimo^{pos}-CSCs divide significantly less than Pimo^{neg}-CSCs and atrial Pimo^{pos}-CSCs possess properties consistent with long-term repopulating stem cells.

Pimo^{pos}-CSCs, SCF and myocardial aging

Myocardial aging manifests itself with the accumulation of poorly contracting, p16^{INK4a}-positive myocytes, despite an increase in their turnover rate and the addition of chronologically younger cells.[3,5,10] The CSCs being activated have lost their phenotypic integrity, a process dictated by telomere dysfunction. CSCs with shortened telomeres divide

frequently, conditioning the characteristics of the myocyte progeny that inherits the partially eroded telomeres of the mother cells.[3,5]

To define whether hypoxic CSCs can be coaxed to reenter the cell cycle and generate mechanically efficient myocytes, two strategies were employed: 26 month-old mice were kept in an atmosphere of 70% O_2 to increase O_2 content in hypoxic CSCs; and stem cell factor (SCF) was delivered to multiple areas of the LV in 26–30 month-old mice to stimulate c-kit, the receptor of SCF, in hypoxic CSCs. Hyperoxia at 70% O_2 was employed since this level of O_2 does not result in symptomatic lung injury.[26]

Hyperoxia decreased by 18% and 19% the fraction of $Pimo^{pos}$-CSCs at 1 and 7 days, respectively. Accordingly, the pool of $Pimo^{neg}$-CSCs increased 29% at 1 day and 32% at 7 days (Online Figure VIIIA and VIIIB), indicating that prolonged hyperoxia did not change the acute effects of this protocol. This strategy has no clinical relevance, but provided preliminary information on the reversibility of the hypoxic state of CSCs in the old heart.

Subsequently, we tested whether c-kit activation by SCF promoted cell cycle reentry of $Pimo^{pos}$-CSCs. Intramyocardial delivery of 2.5 μg SCF did not increase, over a 6 hour period, the blood level of c-kit-positive HSCs (Online Figure IX). A cumulative dose of 1.0 μg was injected in 3–4 separate sites of the LV. Six and 24 hours later, the myocardium was enzymatically dissociated and the proportion of $Pimo^{pos}$- and $Pimo^{neg}$-CSCs was measured by FACS. At 6 hours, $Pimo^{pos}$-CSCs decreased 55% and $Pimo^{neg}$-CSCs increased 97% (Figure 7A). These cells were c-kit-positive and CD45-negative, excluding the contribution of bone marrow cells and mast-cells. The proportion of $Pimo^{pos}$- and $Pimo^{neg}$-CSCs returned to baseline at 24 hours. Thus, SCF has an acute effect on $Pimo^{pos}$-CSCs, a response consistent with the short half-life of this cytokine.[27]

To establish whether SCF led to CSC division, BrdU was given daily and the fraction of BrdU-positive CSCs was measured at 2 days. SCF resulted in a 95% increase in the percentage of BrdU-labeled CSCs (Figure 7B), a value consistent with the 97% increase in $Pimo^{neg}$-CSCs. Thus, SCF activates the growth of $Pimo^{pos}$-CSCs.

The impact of SCF and CSC growth on the anatomy and function of the heart was measured in 26 month-old mice 3 weeks after echo-guided cytokine injection. Importantly, all data were collected blindly. SCF led to a significant decrease in LV diastolic and systolic diameters, together with a dramatic reduction in LV diastolic and systolic volumes. Moreover, the thickness of the anterior and posterior regions of the LV wall consistently increased (Figure 7C), indicating a remarkable change in ventricular remodeling. Invasive cardiac hemodynamics did not differ in control and SCF-treated animals (Online Figure X); however, when the echocardiographic parameters of ventricular anatomy were combined with pressure measurements, a 56% reduction in diastolic anterior ($P<0.008$) and posterior ($P<0.008$) wall stress was found with SCF. Similarly, systolic anterior and posterior wall stress decreased 45% ($p < 0.004$) and 43% ($P<0.006$), respectively (Figure 7D); notably, LV mass-to-chamber volume ratio increased 84% in diastole ($P<0.003$) and 2.2-fold in systole ($P<0.04$) (Figure 7E; Online Figure XI). Thus, division and differentiation of $Pimo^{pos}$-CSCs via c-kit receptor activation results in a dramatic decrease in load on the senescent heart.

Rejuvenation of the senescent heart

To evaluate the formation of cardiomyocytes and CSCs over the 3 week-period following the delivery of SCF, BrdU was administered daily and the percentage of cells positive for the thymidine analog was measured at sacrifice. In comparison with control hearts, the fraction of BrdU-positive myocytes increased 114% following SCF administration (Figure 8A). Interestingly, the percentage of BrdU-labeled CSCs was similar in the two groups,

despite the striking increase in proliferating cells observed at 2 days (see Figure 7B). However, the number of CSCs per mm^3 of myocardium was 32% higher in mice treated with SCF (Figure 8B). Thus, SCF exerted two integrated effects on the senescent heart; repopulated the organ with chronologically younger CSCs and myocytes.

To define the mechanisms of ventricular remodeling, myocyte size, number and the proportion of mononucleated and binucleated cells were determined. Sections, 40 μm thick, were stained by α-sarcomeric actin, connexin 43, and laminin, and the volume of mononucleated and binucleated myocytes and their relative contribution were measured by optical section reconstruction and confocal microscopy (Online Figure XII). These parameters allowed the computation of the number of LV mononucleated and binucleated myocytes. The 29% expansion in LV mass 3 weeks after SCF administration was characterized by a 2.1-fold increase in the number of mononucleated myocytes, which were 55% smaller than in control myocardium (Figure 8C). Conversely, binucleated myocytes decreased 12% in SCF-treated hearts. The volume of binucleated myocytes was similar in both groups of animals, but the number of LV myocytes was 39% higher after treatment with SCF (Figures 8C).

Following SCF, telomere length in newly-formed BrdU-positive myocytes was 75% longer than in preexisting BrdU-negative cells, supporting the notion that regenerated myocytes derived from activation of CSCs, which possessed a younger cell phenotype. In PBS-injected mice, BrdU-positive myocytes carried telomeres only 31% longer than in BrdU-negative cells (Figure 8D). Moreover, in these control hearts, the distribution of telomere lengths in BrdU-positive myocytes was shifted to the left towards shorter values, a phenomenon opposite to that observed in SCF-treated hearts (Figure 8D). As expected, telomere length in BrdU-negative cardiomyocytes did not differ in mice injected with PBS or SCF. Thus, the myocyte progeny derived from growth and differentiation of CSCs with relatively intact telomeres has profound consequences on the cellular composition of the myocardium repopulating partly the heart with a pool of younger cardiomyocytes.

DISCUSSION

Currently, we have little understanding of the etiology of myocardial aging. Rarely, aging has been considered as an independent event and time as the major cause of the senescent cardiac phenotype. Aging has been interpreted as a variable, which cooperates with a variety of diseases, to define the old, poorly functional heart.[28–30] Results in this study suggest that myocardial aging has to be viewed as a stem cell disease, dictated partly by lack of activation of quiescent hypoxic CSCs with intact telomeres, which are present in the senescent heart. This defect has a notable impact on cellular age that differs significantly from chronological age. Physiologically, myocyte renewal in the aged organ is controlled by a class of CSCs with shortened telomeres that, by necessity, is destined to differentiate into myocytes that are chronologically young but phenotypically old, impacting on the myocardium, structurally and functionally. Telomere dysfunction dictates their actual age and mechanical behavior.[10] However, the residual compartment of quiescent phenotypically young CSCs can be stimulated in situ by SCF reversing the aging myopathy. Our findings support the notion that strategies targeting CSCs may interfere with the manifestations of myocardial aging in an animal model. Although caution has to be exercised in the translation of experimental findings to human beings, our observations suggest that the protocol employed here may be beneficial for the aging myopathy improving health-span in the elderly.

CSCs represent a heterogeneous cell category that is particularly apparent in the old heart in which CSCs with extremely short telomeres coexist with CSCs carrying long, intact

telomeres. In analogy to HSCs in the bone marrow,[7] hypoxic CSCs, particularly in the atria, correspond to quiescent long-term label retaining cells that rarely divide, while normoxic CSCs reflect cells that proliferate frequently and generate a specialized progeny. The balance between these two stem cell classes is critical for the regulation of myocardial homeostasis and the preservation of the CSC compartment during the organ lifespan. Aging, however, expands dramatically the pool of quiescent CSCs so that the smaller pool of cycling CSCs sustains cell turnover.

The combination of insulin-like growth factor-1 (IGF-1) and hepatocyte growth factor (HGF) has been shown to activate resident CSCs in the infarcted[31,32] and senescent[3] myocardium resulting in tissue regeneration and restoration of a younger organ phenotype. SCF preferentially operates at the level of hypoxic CSCs with long telomeres, suggesting that this strategy may be important in conditions associated with defects in tissue oxygenation. Moreover, the derived myocyte progeny typically shows long telomeres, a property that is associated with superior contractile performance.[11] However, a direct comparison between IGF-1/HGF and SCF remains to be done to establish potential therapeutic differences of these two modalities of intervention for the injured and old mammalian heart.

Consistent with previous results,[3] the number of CSCs increases with age. However, $p16^{INK4a}$ is also increased together with the level of cell apoptosis. These variables decrease the number of functionally-competent CSCs and the growth reserve of the old myocardium. A similar phenomenon has been observed in the number and activity of HSCs in the bone marrow and crypt stem cells in the small intestine.[33,34] Collectively, our results emphasize the critical role that resident CSCs have in the homeostatic control of the myocardium as a function of age. These findings are in contrast with recent reports questioning the relevance of c-kit-positive CSCs in myocyte turnover and regeneration.[35,36] These differences may reflect the methodology employed and the inherent limitations of lineage tracing studies with promoters of genes encoding contractile proteins.

Although measurements of coronary perfusion in aging mice are lacking, myocardial aging typically induces reduction in coronary blood flow reserve in rats[37] that, together with the decrease in capillary density results in defects in the parameters controlling tissue oxygenation.[12] These age-dependent variables create hypoxic microdomains[38,39] that may account for the increase in the number of inactive CSCs within the myocardium. This view is consistent with our results showing an increase in the diffusion distance for O_2 between hypoxic CSCs and the nearest capillary. The co-localization of Pimo, CAIX and HIF-1α in this subset of CSCs strongly supports the contention of their hypoxic state. The expression of HIF-1α in cardiomyocytes surrounding hypoxic CSCs indicates that these tissue microdomains are in a state of relative hypoxia.

Survival in the hypoxic niche imposes on HSCs the utilization of glycolysis for energy production. This metabolic adaptation is regulated by Meis1 through transcriptional activation of HIF-1α and upregulation of Cripto/GRP78 signaling.[8,17] Whether hypoxic CSCs are characterized by a similar metabolic signature remains to be defined. Anaerobic glycolysis and quiescence reduce the generation of free radicals and the incidence of oxidative DNA damage,[6] while frequent division increases the intracellular content of ROS. The selective advantage associated with limitations in the formation of ROS may be operative in quiescent CSCs, which are characterized by longer telomeres. Moreover, attenuation in oxidative stress opposes the upregulation of $p16^{INK4a}$, replicative senescence and growth arrest, significantly decreased in hypoxic CSCs.

The heterogeneity in CSCs raises the question whether preservation of the number of CSCs within hypoxic and normoxic myocardium depends on the classic modality of self-renewal at the individual cell level, or on a population replacement process.[23] Stem cell self-renewal implies that each niche constitutes an independent unit controlled by an intrinsic homeostatic mechanism that maintains the number of CSCs constant within the niche. The population replacement process entails that the turnover of CSCs is based on a feedback system between hypoxic, quiescent niches and normoxic, active niches with exchange of CSCs, replenishing depleted or dysfunctional niches. Our findings suggest that quiescent and active CSCs may have a cooperative role, pointing to a new model of stem cell turnover in the adult heart.

Although the claim is commonly made that age-associated changes predispose older adults to develop chronic heart failure (CHF), its etiology is essentially unknown. Morbidity and mortality for CHF continue to increase[40] and parallel the extension in median lifespan of the population,[41] pointing to aging as the major risk factor of the human disease. At present, there are 5.1 million patients with CHF in the USA with an annual incidence of 670,000 new cases.[40] And the overwhelming majority of individuals with CHF are 65 years of age or older.[30,42] However, “good” CSCs may be locally activated to replace old, poorly contracting myocytes with young, mechanically powerful cells. Autologous CSCs have recently been introduced in the experimental treatment of patients with CHF with encouraging results.[43–45]

LIMITATIONS

There are some technical aspects that need to be acknowledged since they preclude in part answering a few important questions related to the interpretation of the collected results. Cardiomyocytes with long telomeres can only derive from CSCs with similar or longer telomeres, suggesting that they represent the progeny of hypoxic CSCs, which transiently acquired a normoxic state. This possibility is consistent with the relative increase in normoxic CSCs 6 hours after the injection of SCF. But whether the number of normoxic CSCs increased as a result of a decrease in the pool of hypoxic CSCs was not demonstrated directly. Notably, the cell cycle of CSCs is significantly longer than six hours.[46] Additionally, whether the reconstitution of hypoxic niches following the delivery of TPZ involves normoxic CSCs with initially shorter telomeres was not shown. Moreover, whether these new hypoxic CSCs are able to increase the length of their telomeres with time remains a critical problem to be addressed in future studies.

FACS analysis of freshly isolated CSCs does not allow a valid measurement of the absolute number of any cell population in the myocardium. Too many variables are involved in the process interfering with the evaluation of the aggregate pool. This limitation has precluded us to express FACS data in absolute terms.[47] However, flow cytometry is considered the gold standard for the characterization of the stem cell phenotype.

We do recognize that the measurement of the diffusion distance for oxygen is only one of the factors implicated in the formation of hypoxic niches. Intracellular processes may be more relevant to the myocardium in view of the high number of capillary structures per unit area of tissue. In this study, both components appear to be operative in hypoxic niches as shown by the increase in capillary distance, the lower $\Delta\psi$ and the modest effect of hyperoxia.

We have elected to employ Pimo to obtain data documenting the functional state of CSCs at organ death. However, this approach did not permit us to distinguish whether hypoxia is a transient or a more prolonged cellular phenomenon. This interesting concept will be studied

in the future by sequential injection of nitroimidazole probes with distinct pharmacokinetics and intracellular accumulation rates.[17,48,49]

It might come as a surprise that, despite the high number of capillaries in the myocardium, hypoxic interstitial cells are present within the tissue. Hypoxic stem cell niches are routinely detected in various organs by Pimo together with HIF-1α and its downstream targets.[50] It has recently been shown that HSCs with a hypoxic profile are distributed in the bone marrow independently from the proximity to the endosteal surface and adjacency to vascular profiles.[51]

Supplementary Material

Refer to Web version on PubMed Central for supplementary material.

Acknowledgments

SOURCES OF FUNDING This work was supported by NIH grants.

Nonstandard Abbreviations and Acronyms

CSCs	Cardiac stem cells
ECs	Endothelial cells
α-SA	α-sarcomeric actin
HSCs	Hematopoietic stem cells
SCF	Stem cell factor
Pimo	Pimonidazole
NBT	Nitroblue tetrazolium
TMRE	Tetramethylrhodamine ethyl ester
TPZ	Tirapazamine
HIF-1α	Hypoxia-inducible factor 1-alpha
CAIX	Carbonic anhydrase IX
ROS	Reactive oxygen species
CHF	Chronic heart failure

REFERENCES

1. Urbanek K, Cesselli D, Rota M, Nascimbene A, De Angelis A, Hosoda T, Bearzi C, Boni A, Bolli R, Kajstura J, Anversa P, Leri A. Stem cell niches in the adult mouse heart. Proc Natl Acad Sci USA. 2006; 103:9226–31. [PubMed: 16754876]
2. Hosoda T, D'Amario D, Cabral-Da-Silva MC, Zheng H, Padin-Iruegas ME, Ogorek B, Ferreira-Martins J, Yasuzawa-Amano S, Amano K, Ide-Iwata N, Cheng W, Rota M, Urbanek K, Kajstura J, Anversa P, Leri A. Clonality of mouse and human cardiomyogenesis in vivo. Proc Natl Acad Sci USA. 2009; 106:17169–74. [PubMed: 19805158]
3. Gonzalez A, Rota M, Nurzynska D, Misao Y, Tillmanns J, Ojaimi C, Padin-Iruegas ME, Müller P, Esposito G, Bearzi C, Vitale S, Dawn B, Sanganalmath SK, Baker M, Hintze TH, Bolli R, Urbanek K, Hosoda T, Anversa P, Kajstura J, Leri A. Activation of cardiac progenitor cells reverses the failing heart senescentphenotype and prolongs lifespan. Circ Res. 2008; 102:597–606. [PubMed: 18202313]

4. Kajstura J, Gurusamy N, Ogórek B, Goichberg P, Clavo-Rondon C, Hosoda T, D'Amario D, Bardelli S, Beltrami AP, Cesselli D, Bussani R, del Monte F, Quaini F, Rota M, Beltrami CA, Buchholz BA, Leri A, Anversa P. Myocyte turnover in the aging human heart. Circ Res. 2010; 107:1374–86. [PubMed: 21088285]
5. Torella D, Rota M, Nurzynska D, Musso E, Monsen A, Shiraishi I, Zias E, Walsh K, Rosenzweig A, Sussman MA, Urbanek K, Nadal-Ginard B, Kajstura J, Anversa P, Leri A. Cardiac stem cell and myocyte aging, heart failure, and insulin-like growth factor-1 overexpression. Circ Res. 2004; 94:514–24. [PubMed: 14726476]
6. Mohyeldin A, Garzón-Muvdi T, Quiñones-Hinojosa A. Oxygen in stem cell biology: a critical component of the stem cell niche. Cell Stem Cell. 2010; 7:150–61. [PubMed: 20682444]
7. Takubo K, Goda N, Yamada W, Iriuchishima H, Ikeda E, Kubota Y, Shima H, Johnson RS, Hirao A, Suematsu M, Suda T. Regulation of the HIF-1alpha level is essential for hematopoietic stem cells. Cell Stem Cell. 2010; 7:391–402. [PubMed: 20804974]
8. Miharada K, Karlsson G, Rehn M, Rörby E, Siva K, Cammenga J, Karlsson S. Cripto regulates hematopoietic stem cells as a hypoxic-niche-related factor through cell surface receptor GRP78. Cell Stem Cell. 2011; 9:330–44. [PubMed: 21982233]
9. Frangogiannis NG. Matricellular proteins in cardiac adaptation and disease. Physiol. Rev. 2012; 92:635–688. [PubMed: 22535894]
10. Rota M, Hosoda T, De Angelis A, Arcarese ML, Esposito G, Rizzi R, Tillmanns J, Tugal D, Musso E, Rimoldi O, Bearzi C, Urbanek K, Anversa P, Leri A, Kajstura J. The young mouse heart is composed of myocytes heterogeneous in age and function. Circ Res. 2007; 101:387–99. [PubMed: 17601802]
11. Krohn KA, Link JM, Mason RP. Molecular imaging of hypoxia. J Nucl Med. 2008; 49(Suppl 2): 129S–48S. [PubMed: 18523070]
12. Anversa, P.; Olivetti, G. Cellular basis of physiological and pathological myocardial growth. In: Page, E.; Fozzard, HA.; Solaro, RJ., editors. Handbook of Physiology. Oxford University Press; New York, NY: 2002. p. 75-144.Section 2, The Cardiovascular System, vol. I, The Heart
13. Wilson WR, Hay MP. Targeting hypoxia in cancer therapy. Nat Rev Cancer. 2011; 11:393–410. [PubMed: 21606941]
14. Bearzi C, Rota M, Hosoda T, Tillmanns J, Nascimbene A, De Angelis A, Yasuzawa-Amano S, Trofimova I, Siggins RW, Lecapitaine N, Cascapera S, Beltrami AP, D'Alessandro DA, Zias E, Quaini F, Urbanek K, Michler RE, Bolli R, Kajstura J, Leri A, Anversa P. Human cardiac stem cells. Proc Natl Acad Sci USA. 2007; 104:14068–73. [PubMed: 17709737]
15. Khan M, Meduru S, Mostafa M, Khan S, Hideg K, Kuppusamy P. Trimetazidine, administered at the onset of reperfusion, ameliorates myocardial dysfunction and injury by activation of p38 mitogen-activated protein kinase and Akt signaling. J. Pharmacol. Exp. Ther. 2010; 333:421–429. [PubMed: 20167841]
16. Ljungkvist AS, Bussink J, Kaanders JH, van der Kogel AJ. Dynamics of tumor hypoxia measured with bioreductive hypoxic cell markers. Radiat Res. 2007; 167:127–45. [PubMed: 17390721]
17. Simsek T, Kocabas F, Zheng J, Deberardinis RJ, Mahmoud AI, Olson EN, Schneider JW, Zhang CC, Sadek HA. The distinct metabolic profile of hematopoietic stem cells reflects their location in a hypoxic niche. Cell Stem Cell. 2010; 7:380–90. [PubMed: 20804973]
18. Takubo K, Nagamatsu G, Kobayashi CI, Nakamura-Ishizu A, Kobayashi H, Ikeda E, Goda N, Rahimi Y, Johnson RS, Soga T, Hirao A, Suematsu M, Suda T. Regulation of glycolysis by Pdk functions as a metabolic checkpoint for cell cycle quiescence in hematopoietic stem cells. Cell Stem Cell. 2013; 12:49–61. [PubMed: 23290136]
19. Shin KH, Diaz-Gonzalez JA, Russell J, Chen Q, Burgman P, Li XF, Ling CC. Detecting changes in tumor hypoxia with carbonic anhydrase IX and pimonidazole. Cancer Biol Ther. 2007; 6:70–5. [PubMed: 17172824]
20. Russell J, Carlin S, Burke SA, Wen B, Yang KM, Ling CC. Immunohistochemical detection of changes in tumor hypoxia. Int J Radiat Oncol Biol Phys. 2009; 73:1177–86. [PubMed: 19251089]
21. Kocabas F, Mahmoud AI, Sosic D, Porrello ER, Chen R, Garcia JA, DeBerardinis RJ, Sadek HA. The hypoxic epicardial and subepicardial microenvironment. J Cardiovasc Transl Res. 2012; 5:654–65. [PubMed: 22566269]

22. Denny WA, Wilson WR. Tirapazamine: a bioreductive anticancer drug that exploits tumour hypoxia. Expert Opin Investig Drugs. 2000; 9:2889–901.
23. Li L, Clevers H. Coexistence of quiescent and active adult stem cells in mammals. Science. 2010; 327:542–545. [PubMed: 20110496]
24. Aubert G, Lansdorp PM. Telomeres and aging. Physiol Rev. 2008; 88:557–79. [PubMed: 18391173]
25. Beausejour CM, Campisi J. Ageing: balancing regeneration and cancer. Nature. 2006; 443:404–5. [PubMed: 16957734]
26. Clark JM, Lambertsen CJ. Pulmonary oxygen toxicity: a review. Pharmacol. Rev. 1971; 23:37–133. 1971. [PubMed: 4948324]
27. Lynch DH, Jacobs C, DuPont D, Eisenman J, Foxworthe D, Martin U, Miller RE, Roux E, Liggitt D, Williams DE. Pharmacokinetic parameters of recombinant mast cell growth factor (rMGF). Lymphokine Cytokine Res. 1992; 11:233–43. [PubMed: 1281675]
28. Dimmeler S, Leri A. Aging and disease as modifiers of efficacy of cell therapy. Circ. Res. 2008; 102:1319–1330. [PubMed: 18535269]
29. Hadley EC, Lakatta EG, Morrison-Bogorad M, Warner HR, Hodes RJ. The future of aging therapies. Cell. 2005; 120:557–567. [PubMed: 15734687]
30. Owan TE, Hodge DO, Herges RM, Jacobsen SJ, Roger VL, Redfield MM. Trends in prevalence and outcome of heart failure with preserved ejection fraction. N Engl J Med. 2006; 355:251–259. [PubMed: 16855265]
31. Urbanek K, Rota M, Cascapera S, Bearzi C, Nascimbene A, De Angelis A, Hosoda T, Chimenti S, Baker M, Limana F, Nurzynska D, Torella D, Rotatori F, Rastaldo R, Musso E, Quaini F, Leri A, Kajstura J, Anversa P. Cardiac stem cells possess growth factor-receptor systems that after activation regenerate the infarcted myocardium, improving ventricular function and long-term survival. Circ Res. 2005; 97:663–673. [PubMed: 16141414]
32. Linke A, Müller P, Nurzynska D, Casarsa C, Torella D, Nascimbene A, Castaldo C, Cascapera S, Böhm M, Quaini F, Urbanek K, Leri A, Hintze TH, Kajstura J, Anversa P. Stem cells in the dog heart are self-renewing, clonogenic, and multipotent and regenerate infarcted myocardium, improving cardiac function. Proc Natl Acad Sci USA. 2005; 102:8966–8971. [PubMed: 15951423]
33. Morrison SJ, Wandycz AM, Akashi K, Globerson A, Weissman IL. The aging of hematopoietic stem cells. Nat Med. 1996; 2:1011–1016. [PubMed: 8782459]
34. Potten CS, Martin K, Kirkwood TB. Ageing of murine small intestinal stem cells. Novartis Found Symp. 2001; 235:66–79. [PubMed: 11280034]
35. Hsieh PC, Segers VF, Davis ME, MacGillivray C, Gannon J, Molkentin JD, Robbins J, Lee RT. Evidence from a genetic fate-mapping study that stem cells refresh adult mammalian cardiomyocytes after injury. Nat Med. 2007; 13:970–974. [PubMed: 17660827]
36. Senyo SE, Steinhauser ML, Pizzimenti CL, Yang VK, Cai L, Wang M, Wu TD, Guerquin-Kern JL, Lechene CP, Lee RT. Mammalian heart renewal by pre-existing cardiomyocytes. Nature. 2013; 493:433–436. [PubMed: 23222518]
37. Hachamovitch R, Wicker P, Capasso JM, Anversa P. Alterations of coronary blood flow and reserve with aging in Fischer 344 rats. Am J Physiol. 1989; 256:H66–73. [PubMed: 2912199]
38. Turek Z, Hoofd L, Batra S, Rakusan K. The effect of realistic geometry of capillary networks on tissue PO2 in hypertrophied rat heart. Adv Exp Med Biol. 1992; 317:567–72. [PubMed: 1288175]
39. Rakusan K, Cicutti N, Kazda S, Turek Z. Effect of nifedipine on coronary capillary geometry in normotensive and hypertensive rats. Hypertension. 1994; 24:205–211. 1994. [PubMed: 8039845]
40. Go AS, Mozaffarian D, Roger VL, Benjamin EJ, Berry JD, Borden WB, Bravata DM, Dai S, Ford ES, Fox CS, Franco S, Fullerton HJ, Gillespie C, Hailpern SM, Heit JA, Howard VJ, Huffman MD, Kissela BM, Kittner SJ, Lackland DT, Lichtman JH, Lisabeth LD, Magid D, Marcus GM, Marelli A, Matchar DB, McGuire DK, Mohler ER, Moy CS, Mussolino ME, Nichol G, Paynter NP, Schreiner PJ, Sorlie PD, Stein J, Turan TN, Virani SS, Wong ND, Woo D, Turner MB, American Heart Association Statistics Committee and Stroke Statistics Subcommittee. Heart disease and stroke statistics--2013 update: a report from the American Heart Association. Circulation. 2013; 127:e6–e245. [PubMed: 23239837]

41. Sanderson WC, Scherbov S. Average remaining lifetimes can increase as human populations age. Nature. 2005; 435:811–813. [PubMed: 15944703]

42. Maeder MT, Kaye DM. Heart failure with normal left ventricular ejection fraction. J. Am. Coll. Cardiol. 2009; 53:905–918. [PubMed: 19281919]

43. Bolli R, Chugh AR, D'Amario D, Loughran JH, Stoddard MF, Ikram S, Beache GM, Wagner SG, Leri A, Hosoda T, Sanada F, Elmore JB, Goichberg P, Cappetta D, Solankhi NK, Fahsah I, Rokosh DG, Slaughter MS, Kajstura J, Anversa P. Cardiac stem cells in patients with ischaemic cardiomyopathy (SCIPIO): initial results of a randomised phase 1 trial. Lancet. 2011; 378:1847–57. [PubMed: 22088800]

44. Makkar RR, Smith RR, Cheng K, Malliaras K, Thomson LE, Berman D, Czer LS, Marbán L, Mendizabal A, Johnston PV, Russell SD, Schuleri KH, Lardo AC, Gerstenblith G, Marbán E. Intracoronary cardiosphere-derived cells for heart regeneration after myocardial infarction (CADUCEUS): a prospective, randomized phase 1 trial. Lancet. 2012; 379:895–904. [PubMed: 22336189]

45. Chugh AR, Beache GM, Loughran JH, Mewton N, Elmore JB, Kajstura J, Pappas P, Tatooles A, Stoddard MF, Lima JA, Slaughter MS, Anversa P, Bolli R. Administration of cardiac stem cells in patients with ischemic cardiomyopathy: the SCIPIO trial: surgical aspects and interim analysis of myocardial function and viability by magnetic resonance. Circulation. 2012; 126:S54–64. [PubMed: 22965994]

46. Ferreira-Martins J, Ogórek B, Cappetta D, Matsuda A, Signore S, D'Amario D, Kostyla J, Steadman E, Ide-Iwata N, Sanada F, Iaffaldano G, Ottolenghi S, Hosoda T, Leri A, Kajstura J, Anversa P, Rota M. Cardiomyogenesis in the developing heart is regulated by c-kit-positive cardiac stem cells. Circ Res. 2012; 110:701–715. [PubMed: 22275487]

47. Mandy F, Brando B. Enumeration of absolute cell counts using immunophenotypic techniques. Curr Protoc Cytom. 2001; Chapter 6(Unit 6.8)

48. Ljungkvist AS, Bussink J, Rijken PF, Raleigh JA, Denekamp J, Van Der Kogel AJ. Changes in tumor hypoxia measured with a double hypoxic marker technique. Int J Radiat Oncol Biol Phys. 2000; 48:1529–1538. [PubMed: 11121659]

49. Bennewith KL, Durand RE. Quantifying transient hypoxia in human tumor xenografts by flow cytometry. Cancer Res. 2004; 64:6183–6189. [PubMed: 15342403]

50. Dalloul A. Hypoxia and visualization of the stem cell niche. Methods Mol Biol. 2013; 1035:199–205. [PubMed: 23959993]

51. Nombela-Arrieta C, Pivarnik G, Winkel B, Canty KJ, Harley B, Mahoney JE, Park SY, Lu J, Protopopov A, Silberstein LE. Quantitative imaging of haematopoietic stem and progenitor cell localization and hypoxic status in the bone marrow microenvironment. Nat Cell Biol. 2013; 15:533–543. [PubMed: 23624405]

Novelty and Significance

What Is Known?

- In the myocardium, c-kit-positive cardiac stem cells (CSCs) are clustered in interstitial microdomains with the properties of stem cell niches.
- With aging, the fraction of CSCs expressing the senescence-associated protein $p16^{INK4a}$ increases, reducing the number of functionally-competent CSCs.
- A pool CSCs with long telomeres persists in the senescent myocardium.

What New Information Does This Article Contribute?

- CSC niches are functionally heterogeneous and are composed of active and quiescent niches.
- Cellular hypoxia preserves the quiescent undifferentiated state of CSCs, which are characterized by long telomeres, low expression of $p16^{INK4a}$, and a high growth reserve, typically present in CSCs with a young cellular phenotype.
- Hypoxic CSC niches increase with age but can be activated by stem cell factor (SCF) generating a large progeny of chronologically and phenotypically young cardiomyocytes.

Currently, we have little understanding of the etiology of myocardial aging. Rarely, aging has been considered as an independent event and time as the major cause of the senescent cardiac phenotype. Results in this study suggest that myocardial aging has to be viewed as a stem cell disease, dictated partly by lack of activation of quiescent hypoxic CSCs with intact telomeres, which are present in the senescent heart. This defect has a notable impact on cellular age that differs significantly from chronological age. Myocyte renewal in the aged organ is controlled by a class of CSCs with shortened telomeres that differentiate into old poorly contracting myocytes. However, the residual compartment of quiescent phenotypically young CSCs can be stimulated in situ by SCF reversing the aging myopathy. Our findings support the notion that strategies targeting CSCs may interfere with the manifestations of myocardial aging in an animal model.

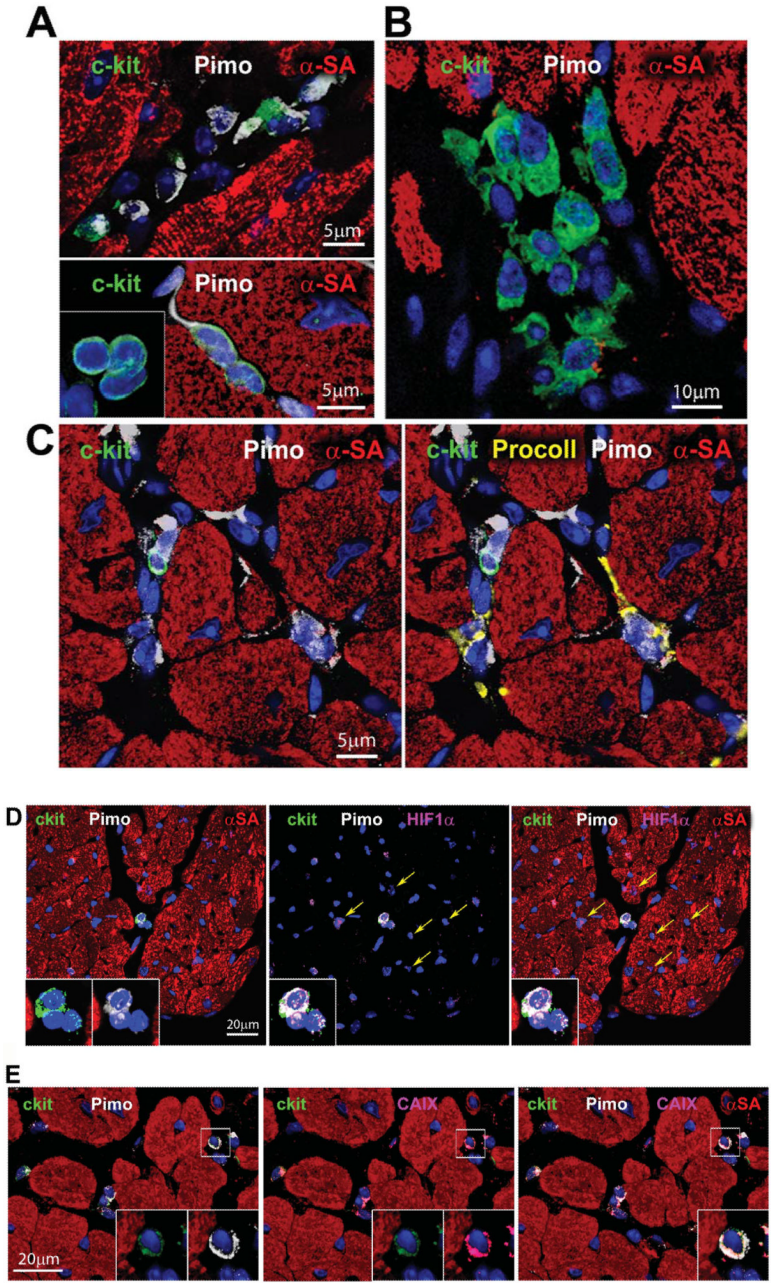

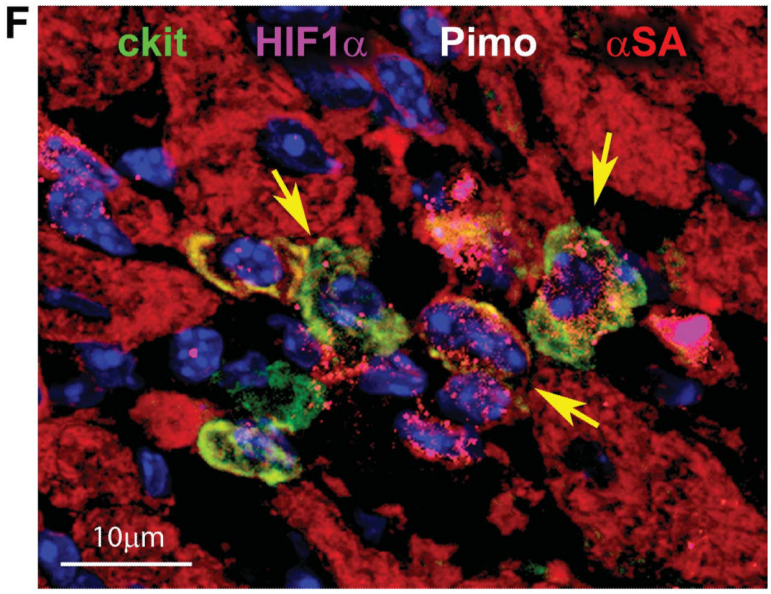

Figure 1. Hypoxic and normoxic CSC niches

A and **B**: Three examples of Pimo^{pos} (**A**, white) and one example of Pimo^{neg} (**B**) c-kit-positive CSCs (green). Myocytes are stained by α-sarcomeric actin (α-SA, red). **C**: Pimo^{pos} (white) c-kit-positive CSCs are surrounded by Pimo^{pos} fibroblasts (procollagen, yellow) and Pimo^{neg} cardiomyocytes. **D**: HIF-1α (magenta) is present in Pimo^{pos}-CSCs and Pimo^{neg} cardiomyocytes (α-SA, red; arrows). The area in the rectangle is shown at higher magnification in the insets. **E**: CAIX (magenta) is restricted to Pimo^{pos}-CSCs. Labeling for c-kit, Pimo, and CAIX are shown at higher magnification in the insets. **F**: HIF-1α (magenta) is present in a cluster of Pimo^{neg}-CSCs (arrows).

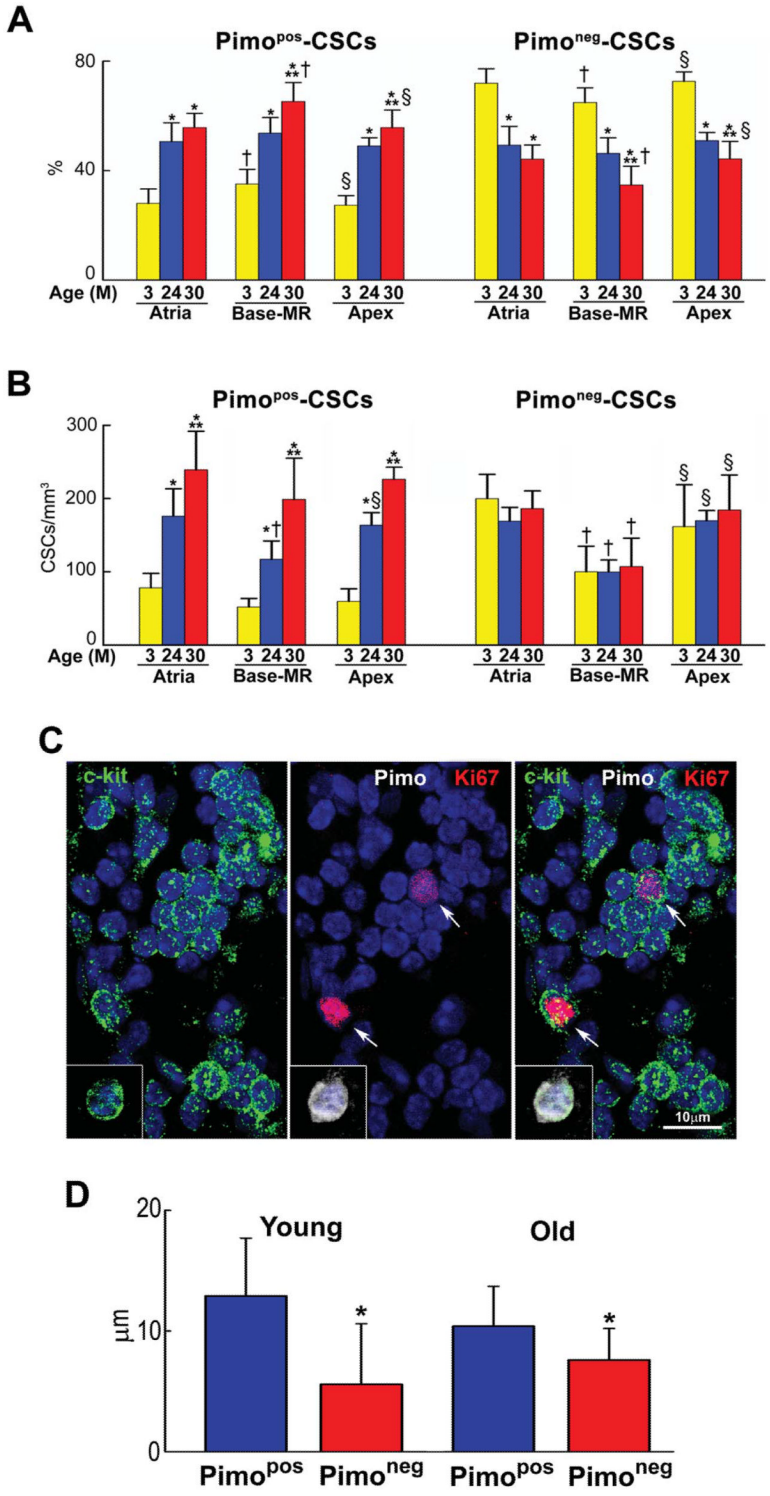

Figure 2. Aging increases the number of hypoxic CSCs

A: Fraction of Pimo^{pos}- and Pimo^{neg}-CSCs with age. M, months. *,**,†,§$P<0.05$ vs. 3M, 24M, Atria, Base-MR, respectively. **B**: Number of Pimo^{pos}- and Pimo^{neg}-CSCs per mm^3/ myocardium. For statistics and symbols see above. **C**: Myocardial niche composed of Pimo^{neg}-CSCs; two CSCs are labeled by Ki67 (red, arrows). Inset: Pimo^{pos}-CSC used as

positive control for Pimo. **D**: Diffusion distance for O_2 in $Pimo^{pos}$- and $Pimo^{neg}$-CSCs in mice at 3M (young) and 24–30M (old) of age. *$p < 0.05$ vs. $Pimo^{pos}$.

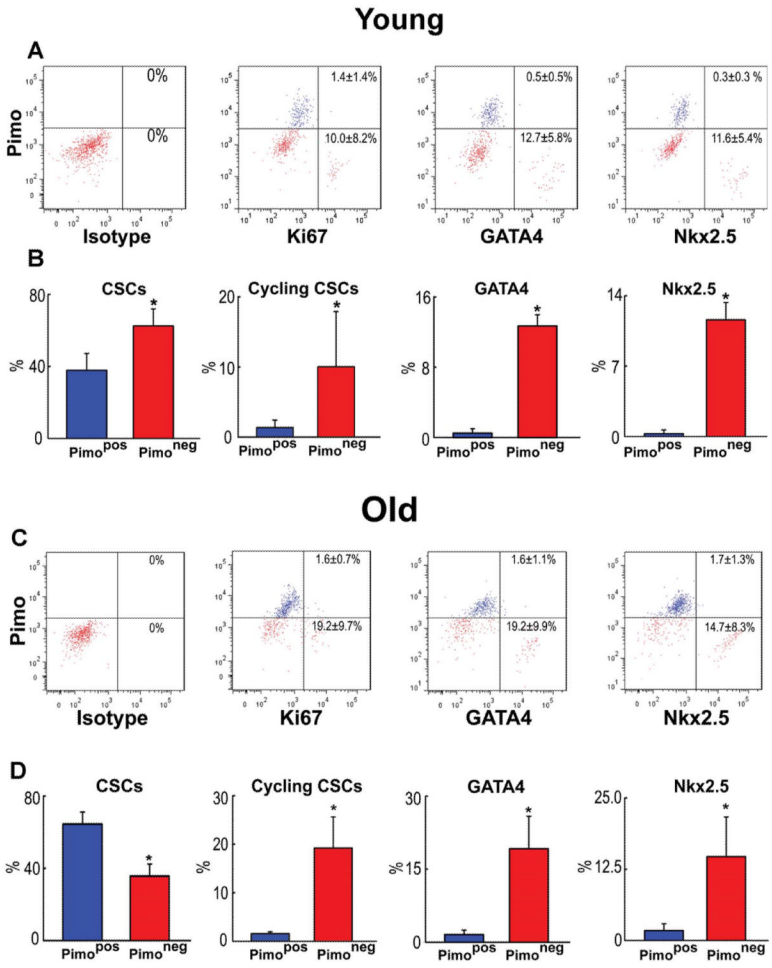

Figure 3. Pimo^{pos}- and Pimo^{neg}-CSCs in the young and old myocardium

A through **D**: Bivariate distribution of Pimo, Ki67, GATA4 and Nkx2.5 in CSCs from young (**A**: 3M) and old (**C**: 30M) hearts. Quantitative results in young (**B**) and old (**D**) are shown as mean±SD. **P*<0.05 vs. Pimo^{pos}.

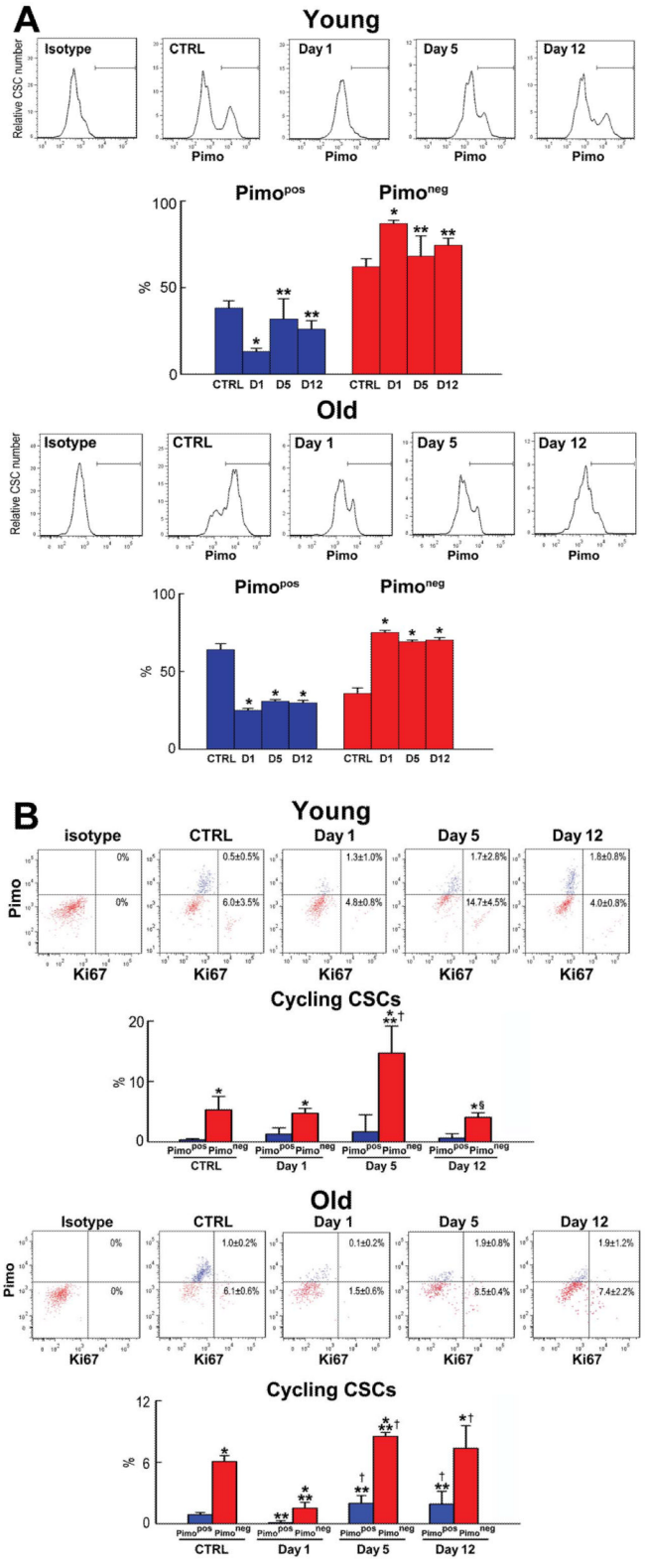

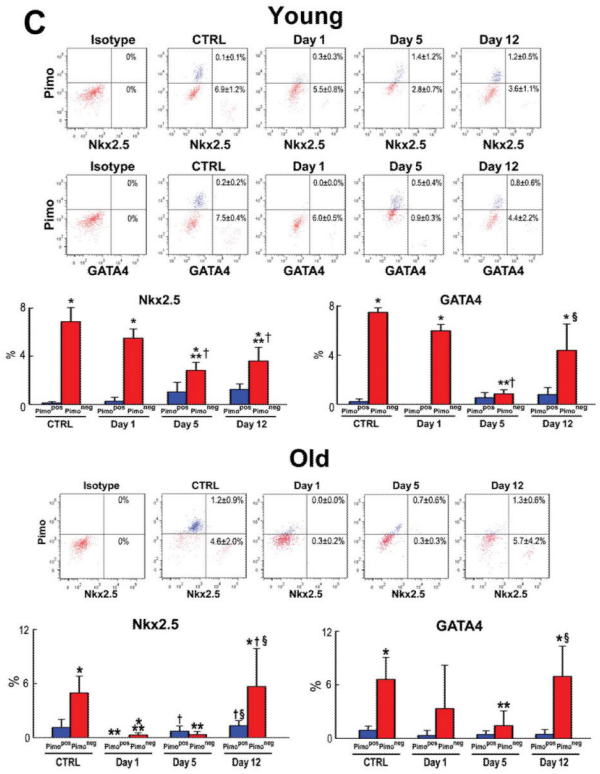

Figure 4. TPZ treatment

A: Distribution of Pimo^{pos}- and Pimo^{neg}-CSCs at baseline (untreated control, CTRL) and at day 1, day 5, and day 12 in TPZ-treated young (3M) and old (30M) mice. The horizontal line indicates the population of Pimo^{pos}-CSCs. *,**$p < 0.05$ vs. CTRL, and day 1, respectively. **B**: Bivariate distribution of Pimo and Ki67 in CSCs from young (3M) and old (30M) TPZ-treated mice. *,**,†,§$p < 0.05$ vs. Pimo^{pos}, CTRL, day 1, and day 5, respectively. **C**: Bivariate distribution of Pimo, Nkx2.5, and GATA4 in CSCs from young (3M) and old (30M) TPZ-treated mice. For statistics and symbols see above.

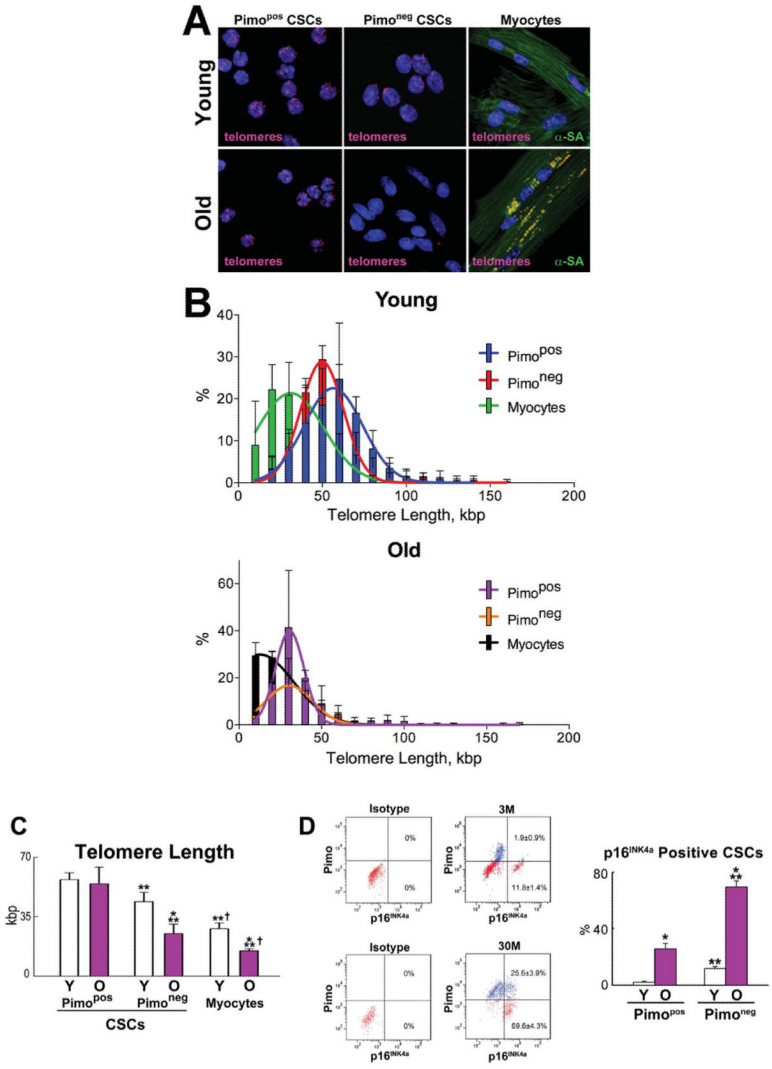

Figure 5. CSC age

A: Pimo^{pos}- and Pimo^{neg}-CSCs were sorted by FACS, and LV myocytes were freshly isolated. Confocal images of CSC preparations and myocytes; telomere length was measured by Q-FISH in young (3M) and old (30M) mice. Individual telomeres are shown by magenta dots. Yellow dots in old cardiomyocytes correspond to lipofuscin. **B** and **C**: Distribution of telomere lengths (**B**) and their average values (**C**) in Pimo^{pos}- and Pimo^{neg}-CSCs and myocytes. *,**,†P<0.05 vs. Y, Pimo^{pos}, Pimo^{neg}, respectively. **D**: Bivariate distribution of Pimo and p^{16INK4a} in CSCs from young (Y: 3M) and old (O: 30M) mice. *,**P<0.05 vs. Y and Pimo^{pos}, respectively.

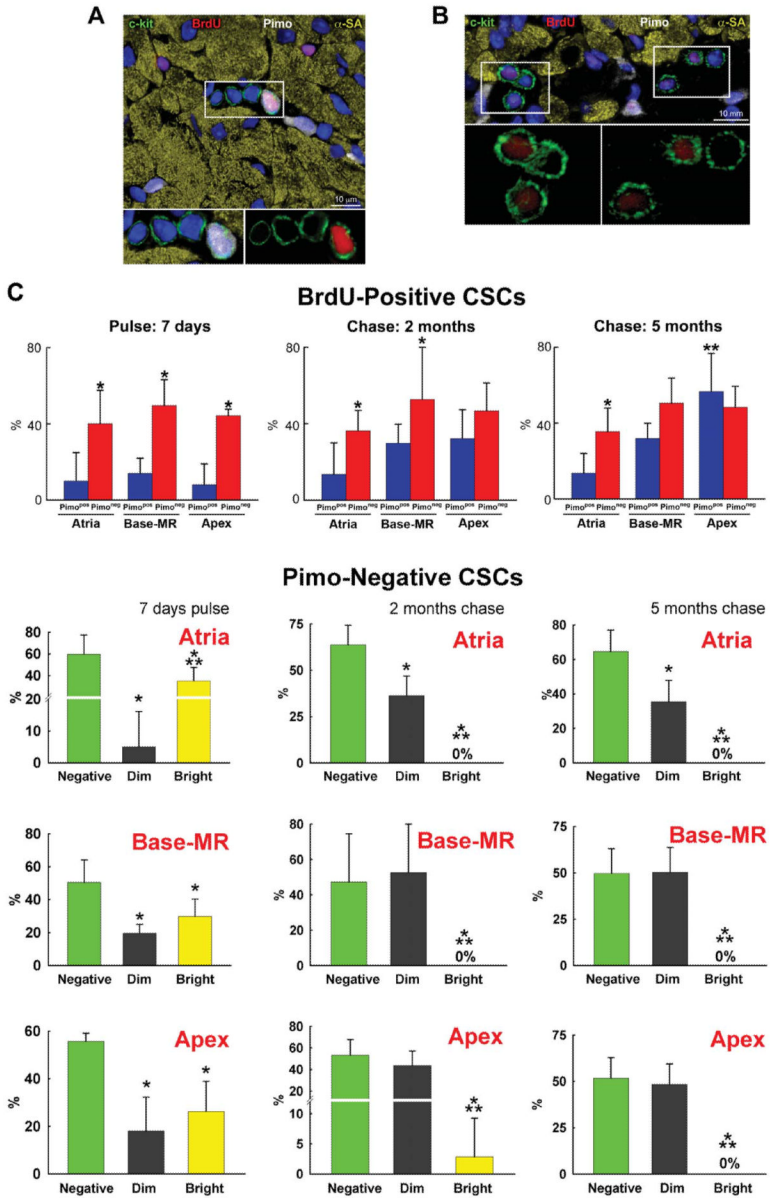

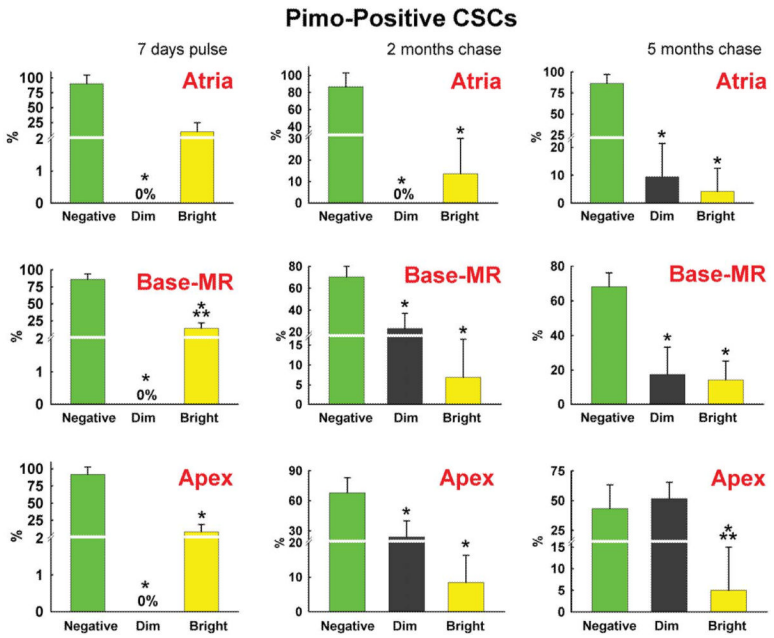

Figure 6. Long-term BrdU label retaining assay

A: Myocardial niche containing 4 c-kit-positive CSCs (green); one CSC is Pimo^{pos} and brightly labeled by BrdU (white-red); c-kit, Pimo, and BrdU are illustrated separately in the insets. **B**: Myocardial section containing 6 c-kit-positive CSCs (green); all CSCs are Pimo^{neg}, and 4 are dimly labeled by BrdU (red); c-kit and BrdU are illustrated separately in the insets. **C**: Percentage of BrdU-positive Pimo^{pos}-CSCs (blue bars) and Pimo^{neg}-CSCs (red bars) at the end of pulse (7 days), and following 2 and 5 month-chase period. **D** and **E**: Distribution of BrdU in Pimo^{neg}-CSCs (**D**) and Pimo^{pos}-CSCs (**E**) in the atria, Base-MR, and apex at the end of pulse (7 days), and following 2 and 5 month-chase period: BrdU-negative CSCs (green bars), BrdU-dim CSCs (black bars), and BrdU-bright CSCs (yellow bars). **C** through **E**: Results are shown as mean±SD. In **C**: *,**$P<0.05$ vs. Pimo^{pos}, and Pimo^{pos} in the atria, respectively. In **D** and **E**: *,**$P<0.05$ vs. BrdU-negative and BrdU-dim CSCs, respectively.

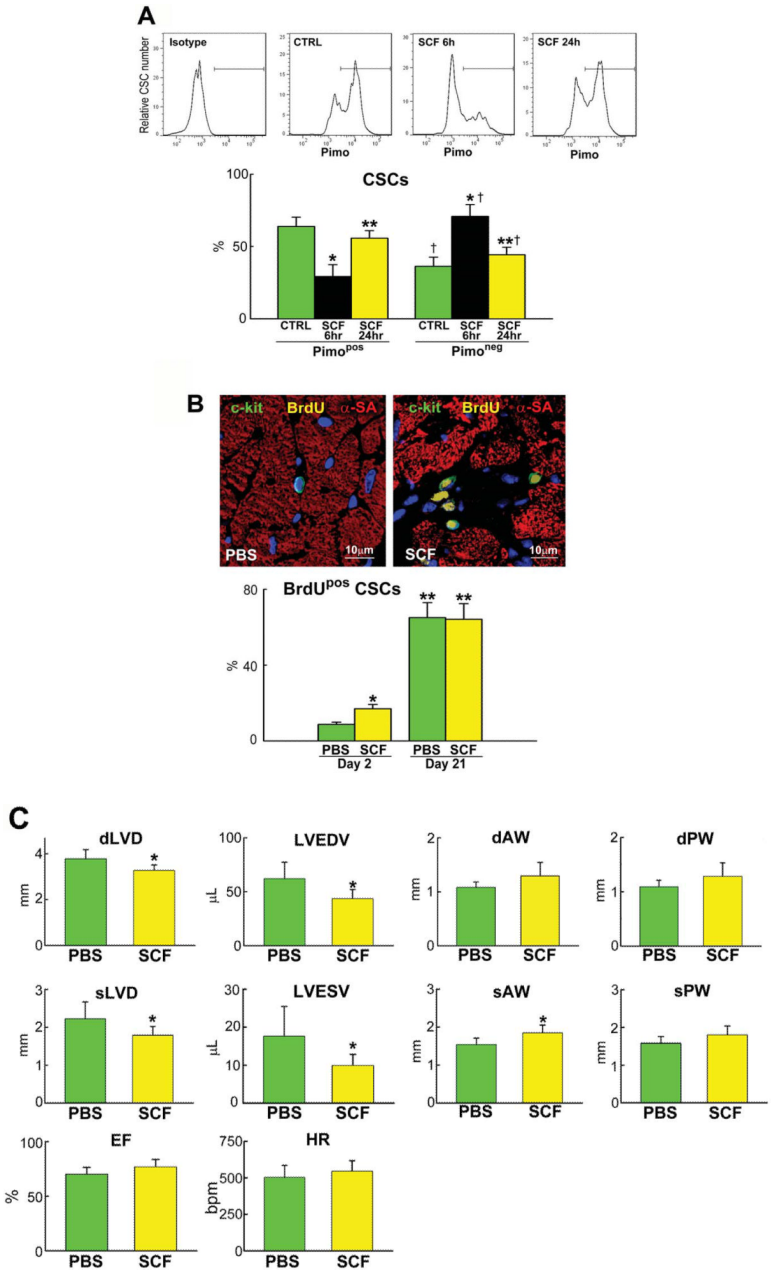

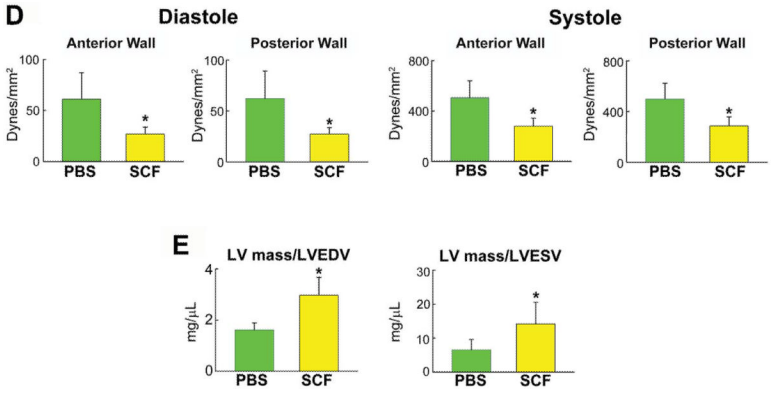

Figure 7. SCF activate Pimo^{pos}-CSCs

A: Mice 26–30 month-old: distribution of Pimo^{pos}- and Pimo^{neg}-CSCs at baseline (CTRL) and 6 and 24 hours (h) after SCF injection. The horizontal line indicates the population of Pimo^{pos}-CSCs. CTRL, green bars; 6 h, black bars; 24 h, yellow bars. *,**,†P<0.05 vs. CTRL, SCF injection at 6 h, and Pimo^{pos}-CSCs, respectively. **B**: Mice 26–30 month-old: BrdU labeling (yellow) in c-kit-positive (green) CSCs in control (PBS) and SCF-treated LV. Myocytes are stained by α-SA (red). PBS, green bars; SCF, yellow bars. *,**P<0.05 vs. PBS at 2 days, and vs. PBS and SCF at 2 days, respectively. **C** through **E**: Echocardiographic parameters (**C**), wall stress (**D**) and LV mass-to-chamber volume ratio (**E**) in control (PBS, green bars) and SCF-treated (yellow bars) mice. *P<0.05 vs. PBS. dLVD, diastolic LV diameter; LVEDV, LV end-diastolic volume; dAW, diastolic anterior wall thickness; dPW, diastolic posterior wall thickness; sLVD, systolic LV diameter; LVESV, LV end-systolic volume; sAW, systolic anterior wall thickness; sPW, systolic posterior wall thickness; EF, ejection fraction; HR, heart rate.

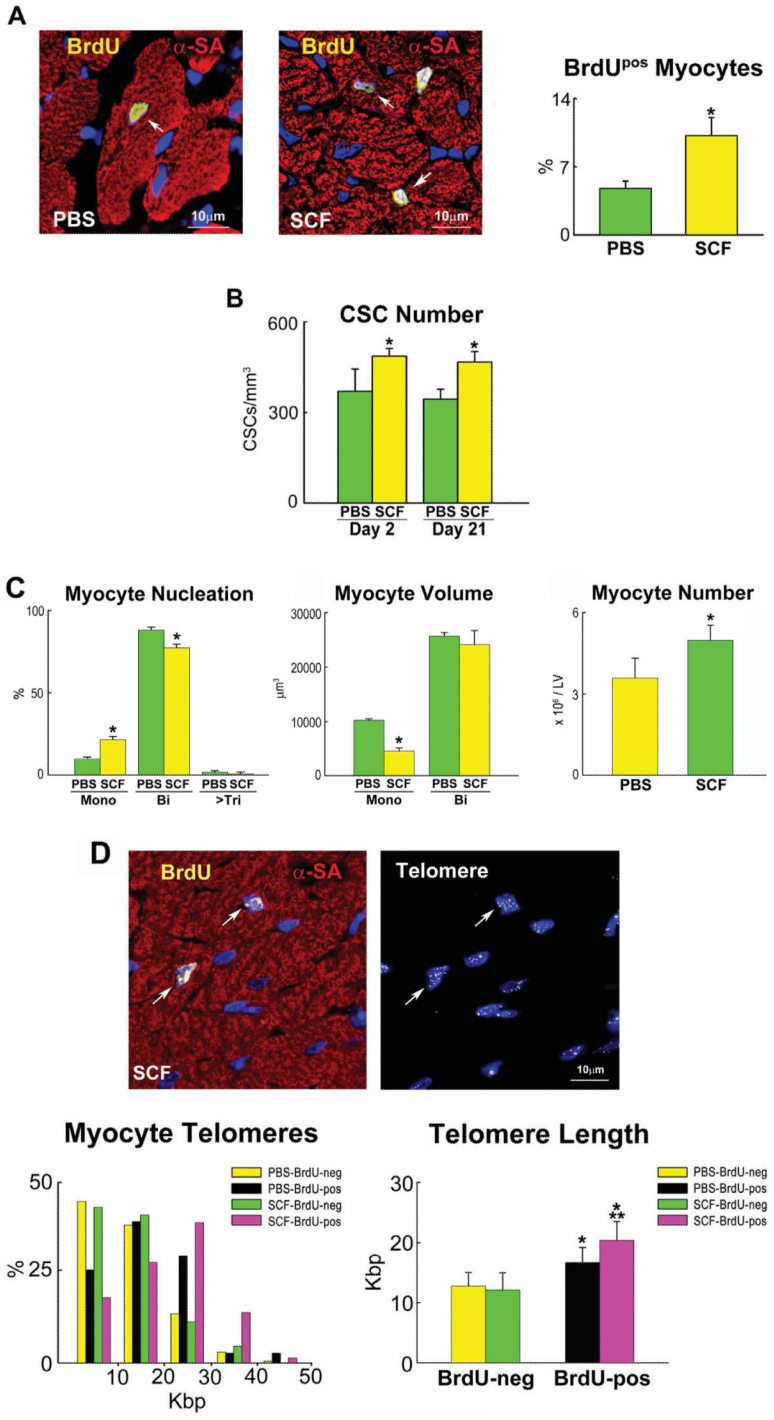

Figure 8. SCF and Myocyte Regeneration

A: Mice 26–30 month-old: BrdU labeling (yellow) in cardiomyocytes (α-SA, red) of control (PBS) and SCF-treated hearts. Data are shown as mean±SD. PBS, green bars; SCF, yellow bars. **P*<0.05 vs. PBS. **B**: CSCs per mm^3 of myocardium. **P*<0.05 vs. PBS. **C**: Proportion, volume and number of mononucleated and binucleated myocytes in the LV of control (PBS) and SCF-treated hearts. **P*<0.05 vs. PBS. **D**: Telomere length measured by Q-FISH in BrdU-positive (yellow nuclei; arrows) and negative (DAPI, blue) myocytes. Distribution

and average values of telomeres in BrdU-positive and BrdU-negative myocytes in mice injected with PBS or SCF. *,**$P<0.05$ vs. BrdU-negative myocytes and vs. BrdU-positive myocytes treated with PBS, respectively.